

ORIGINAL RESEARCH

Comparative analysis of dynamic contrast-enhanced MRI, dynamic contrast-enhanced CT, and their combination for adrenal tumor diagnosis in men

Minghui Yan¹, Yanan Wang¹, Lianghong Jiao^{1,*}

¹Medical Imaging Center, Ningbo
Yinzhou No.2 Hospital, 315192 Ningbo,
Zhejiang, China

*Correspondence
lh_jiao0221@163.com
(Lianghong Jiao)

Abstract

This study aimed to compare the diagnostic efficacy of dynamic contrast-enhanced computed tomography (CT), dynamic contrast-enhanced Magnetic Resonance Imaging (MRI) and their combination in diagnosing adrenal tumors. 68 patients with adrenal tumors admitted to the hospital from December 2019 to December 2020 were selected. MRI and CT plain scans were performed on all patients, as well as dynamic contrast-enhanced imaging. As the gold standard for evaluating diagnostic efficacy, dynamic contrast-enhanced CT, dynamic contrast-enhanced MRI, and their combination were compared with pathological examination results. To compare diagnostic method differences, receiver operating characteristic (ROC) curves were plotted. MRI contour rates at each delay point were significantly higher in adenoma patients than non-adenoma patients ($p < 0.05$). CT contour rates at each delay point were also significantly higher in adenoma patients than non-adenoma patients ($p < 0.05$). The sensitivity, accuracy and negative predictive value of the combined diagnostic examination were significantly higher than individual examinations ($p < 0.05$). Based on ROC curve analysis, dynamic contrast-enhanced MRI, dynamic contrast-enhanced CT, and the combined diagnostic had an area under the curve (AUC) of 0.818 (95% Confidence Interval (CI): 0.696–0.940), 0.827 (95% CI: 0.706–0.949), and 0.908 (95% CI: 0.769–1.019), respectively. The combined diagnosis showed the largest AUC with significant differences ($p < 0.05$). The overall model quality analysis showed that the model values of single and combined indicators were greater than 0.5, and the highest value of the combined index was 0.80. In summary, the combination of dynamic-enhanced CT and dynamic-enhanced MRI is more effective at diagnosing adrenal tumors than either technique alone. Combination diagnoses can assist in diagnosing and treating adrenal tumors with high clinical application value.

Keywords

Dynamic contrast-enhanced CT; Dynamic contrast-enhanced MRI; Combined examination; Adrenal tumor; Diagnostic efficacy

1. Introduction

Adrenal tumors develop in the adrenal glands, which are endocrine glands [1]. Adrenal glands are a pair of small glands located above the kidneys. They secrete various hormones, such as epinephrine, norepinephrine and cortisol, which play crucial roles in metabolism, stress response and homeostasis [2]. Approximately 2% to 10% of people can be found with adrenal tumors during a physical examination [3]. They usually do not cause symptoms, but some metastatic tumors may. In adrenal tumors, most adenomas do not require surgery, whereas non-adenomas (which may be metastatic) do [4]. Medical imaging is the main method used today for determining the nature of tumors, which is a non-invasive test [5]. For incidentally detected adrenal masses, the American College of

Radiology recommends making a preliminary assessment by imaging features, including the size, density and morphology of the mass. CT and MRI are widely used in the clinic, but they have certain limitations in qualitative diagnosing adrenal tumors [6]. As of now, dynamic-enhanced CT and dynamic-enhanced MRI are superior in differential diagnosis. With clear images, quantitative measurements of functional parameters, multiplanar and three-dimensional reconstruction, and non-invasiveness, they can improve the accuracy of tumor diagnosis and the selection of appropriate treatment options [7]. However, CT and MRI combined diagnosis of adrenal tumors has been only studied in a few clinical trials. Efficacy of diagnosis using both methods requires further investigation and validation [8]. This study evaluated the diagnostic efficacy of dynamic-enhanced CT, dynamic-enhanced MRI, and their

combined examinations on adrenal tumors in patients admitted to our hospital.

2. Information and methods

2.1 Clinical data

A retrospective analysis of 68 adrenal tumor patients admitted to the hospital from December 2019 to December 2020 was conducted. Patients ranged in age from 30 to 62 years, with a mean age of (44.35 ± 4.06) years; all subjects were male. We analyzed 56 patients with adenomas and 12 patients without adenomas based on their pathological types.

2.1.1 Inclusion criteria

- (1) Pathologically confirmed adrenal tumor patients who met diagnostic criteria.
- (2) Patients underwent dynamic-enhanced CT scans.
- (3) Age over 18.
- (4) Patients with complete clinical imaging data.

2.1.2 Exclusion criteria

- (1) Patients with combined cardiac, hepatic, renal and other systemic functional abnormalities.
- (2) Pregnant women/lactating mothers.
- (3) Patients with combined psychiatric system diseases.
- (4) Patients with limited mobility.

2.2 Examination methods

Study subjects were admitted to the hospital and underwent dynamic-enhanced CT and MRI examinations using SOMATOM Magnetom Skyra 3.0 T (Siemens Shenzhen Co., Ltd., Shenzhen, China) and SOMATOM Emotion 6 (Siemens Beijing Co., Ltd., Beijing, China). All examination operations were performed by the same group of staff.

2.2.1 MRI scanning and dynamic enhancement

Set the echo time (TR) to 100 ms, emission time (TE) to 4.2 ms, time to 15 s, layer thickness to 5 mm, and layer spacing to 1 mm. Depending on the unique circumstances, these values can be modified accordingly. Place the patient in a supine position with both upper limbs elevated above the head. Patient was instructed to hold his breath and wear headphones before beginning the scan. The scanning range encompassed the renal hilum from the top edge of T12 to the lower edge of L1. First, a standard Spin Echo (SE) sequence scan was performed, and T1 weighted image (T1WI) and T2WI axial locations were requested. An axial gradient echo sequence scan was performed after the scan to determine the greatest tumor cross-section.

A dynamic enhancement scan was performed on a patient at the end of the plain scan. As the contrast agent, gadopentate monoglucosamine injection (Shanghai Hengrui Medicine Co., Ltd; approval number: State Drug License H20200004; specification: 0.5 mmol/mL, 10 mL/pack, Shanghai, China) was used. We performed dynamic enhanced imaging 1, 5 and 7 min after injecting 0.01 mmol/kg. The enhancement scanning parameters were as follows: 3D-FLASH continuous

multi-phase non-interval scanning, with the following specific parameters: layer thickness 2 mm, TE: 1~4 ms, TR: 4~8 ms, flip angle 13°, matrix: 400 × 260, Field of View (FOV): 40 cm × 40 cm, number of excitation (NEX): 1. As part of the scanning process, subcutaneous fat signals were observed and recorded in detail. The average value is determined by multiple tests (at least 3 tests).

2.2.2 CT scanning and dynamic enhancement

Patients were given the contrast agent 2% compound pantethine glucosamine (Beijing Shuangjitai Pharmaceutical Co., Ltd; Approval No.: State Pharmaceutical License H10990147; Specification: 2% compound pantethine glucosamine injection, 50 mL/vial, Shanghai, China) orally 30 min and 1 minute before the examination. Specifications of the equipment have been changed to set layer thickness at 5 mm, layer pitch at 1.5 mm, and speed at 1 layer/s. The parameters could be modified according to the situation. The patient remained a supine posture during a CT scan of the adrenal region. During scanning, the position, size and form of the patient's localized lesions were carefully noted, as well as the contours, interior density, and whether or not the borders were clear.

Dynamic enhanced CT scan was performed on three consecutive sections with a relatively large central cross-sectional area of the tumor found on the plain scan. Iohexol injection (Shanghai Hengrui Medicine Co., Ltd; approval number: GBP H20030015; specification: 0.05 g/mL, 10 mL/branch, Shanghai, China) was given to patients *via* a high-pressure syringe (2.5 mL/s). The enhancement scanning parameters were as follows: 3D-FLASH continuous multi-phase non-interval scanning, with the following specific parameters: layer thickness 2 mm, TE: 1~4 ms, TR: 4~8 ms, flip angle 13°, matrix: 400 × 260, FOV: 40 cm × 40 cm, NEX: 1. Dynamic enhancement scans were performed 1, 5 and 7 min after the injection. As part of the scan, the location, size and morphology of the tumor were assessed and recorded as well as the density, boundary and enhancement status of the tumor. Multiple tests were used to determine the average value (at least 3 tests).

2.3 Observation indicators

Dynamic-enhanced CT, dynamic-enhanced MRI, and a combined examination of the two were compared with the pathological examination of the patients, and the results validated the diagnosis.

(1) The contour rate of each delay point in patients with and without adenomas was compared.

① Dynamic-enhanced MRI contour rate = (maximum signal value after enhancement/fat signal value at the same level – signal value after enhancement/fat signal value at the same level)/(maximum signal value after enhancement/fat signal value at the same level);

② Dynamic-enhanced CT contour rate = (parenchymal CT value – delayed CT value)/(parenchymal CT value – plain CT value).

(2) A group of professional imaging physicians with 10 years of clinical experience interpreted dynamic-enhanced CT and dynamic-enhanced MRI results. Findings were based on unified viewpoints; if two physicians could not agree, a third

physician was consulted to obtain conclusions.

(3) Three diagnostic methods were examined and their efficacy compared; sensitivity, specificity, accuracy, positive predictive value, and negative predictive value. Receiver Operating Characteristic Curves (ROC curves) were used to evaluate the diagnostic accuracy of the two methods.

① Sensitivity = number of true positive cases/(number of true positive cases + number of false negative cases) \times 100%;

② Specificity = number of true negative cases/(number of true negative cases + number of false positive cases) \times 100%;

③ Accuracy = (number of true positive cases + number of true negative cases)/total number of cases \times 100%;

④ Positive predictive value = number of true positive cases/(number of true positive cases + number of false positive cases) \times 100%;

⑤ Negative predictive value = number of true negative cases/(number of true negative cases + number of false negative cases) \times 100%.

2.4 Statistical analysis methods

Data were analyzed and processed by SPSS 27.0 (International Business Machines Corporation, Armonk, NY, USA). Measurement data were presented as mean ($\bar{x} \pm s$), and comparison was made by *t*-test. Count data were presented as cases (%), and the comparison was made by χ^2 . $p < 0.05$ indicates statistically significant differences.

ROC curves were plotted using SPSS to further compare the two diagnostic methods.

3. Results

3.1 Comparison of MRI contour rates at each delay point between adenoma and non-adenoma patients

MRI contour rates at each delay point were significantly higher in adenoma patients than non-adenoma patients ($p < 0.05$) (Table 1).

3.2 Comparison of CT contour rates at each delay point between adenoma and non-adenoma patients

CT contour rates at each delay point were significantly higher in adenoma patients than non-adenoma patients ($p < 0.05$) (Table 2).

3.3 Comparison of the conformity and diagnostic efficacy of the three examinations with the pathologic results

The sensitivity, accuracy and negative predictive value of the combined diagnostic examinations were significantly higher than individual examinations ($p < 0.05$) (Tables 3,4).

3.4 ROC curve analysis

Areas under the ROC curves and their 95% CIs for dynamic-enhanced MRI, dynamic-enhanced CT, and the combined examination were 0.818 (95% CI: 0.696–0.940), 0.827 (95% CI:

0.706–0.949), and 0.908 (95% CI: 0.769–1.019), respectively. The combined diagnostics showed the largest area under the ROC curves with significant differences, suggesting the combined diagnosis was superior (Tables 5,6 and Fig. 1).

3.5 Overall model quality results

The overall model quality results show that single indicators and joint indicators have all been found to be >0.5 , indicating that all three diagnostic methods have high diagnostic values for adrenal tumors. Among these, the joint index has the highest model value, which indicates the greatest predictive value (Fig. 2).

4. Discussion

In general, kidney cancer is more prevalent in men than in women. Epidemiologic data and clinical observations indicate that kidney cancer incidence is usually twice as high in men as in women. There could be various factors contributing to this gender gap, including physiology, lifestyle, risk factors for the disease, and hormone levels. Therefore, male subjects were selected for this study, which may aid in the understanding of disease characteristics in medical research and clinical practice. Despite their commonness, adrenal tumors are challenging to diagnose early due to their specific location, which results in no obvious symptoms early in the disease course [9]. Adrenal gland tumors, including metastatic tumors, pheochromocytoma and cortical carcinoma are usually more serious, with a high mortality rate. Therefore, early diagnosis and treatment of adrenal tumors is necessary [10]. Currently, image-guided or surgical adrenal biopsy enables definitive adrenal tumor identification and diagnosis. It is, however, a highly invasive procedure [11].

With the advancement of imaging technology, MRI and CT examinations has become an option for diagnosing adrenal tumors [12]. In particular, dynamic-enhanced MRI and CT offer more clinical advantages. Studies [13, 14] found CT and MRI examination methods to be effective for determining adenomatous locations, sizes and morphologies, and to be valuable in diagnosing adenomas. This indicates that CT and MRI can be used for adrenal tumor clinical diagnosis. Currently, it is rare to find clinical studies using dynamic-enhanced CT and dynamic-enhanced MRI together to diagnose adrenal adenomas. This study addresses and analyzes this problem.

This study showed that MRI and CT contouring rates at all delay points were significantly higher in adenoma patients than in non-adenoma patients ($p < 0.05$). As a result, dynamic-enhanced CT and dynamic-enhanced MRI both were found to be diagnostically useful in identifying adenomas and non-adenomas. As explained by [15]: there is a significant correlation between the contour rate and the degree of tumor enhancement, which measures the efficiency of removing the contrast agent from the tumor. Blood supply is also positively correlated with tumor enhancement. Thus, the degree of enhancement is higher for non-adenomas, which have better blood supplies and more intratumoral blood vessels, while it is lower for adenomas, which have fewer intratumoral blood

TABLE 1. Comparison of MRI contour rates at each delay point between adenoma and non-adenoma patients ($\bar{x} \pm s$).

Type of tumor	n	1 min	5 min	7 min
Adenoma	56	13.58 \pm 1.25	36.54 \pm 3.16	39.65 \pm 3.06
Non-adenoma	12	7.68 \pm 0.65	14.98 \pm 1.34	18.96 \pm 1.51
<i>t</i> value	—	15.832	23.084	22.737
<i>p</i> value	—	<0.001	<0.001	<0.001

TABLE 2. Comparison of CT contouring rates at each delay point between adenoma and non-adenoma patients ($\bar{x} \pm s$).

Type of tumor	n	1 min	5 min	7 min
Adenoma	56	14.36 \pm 1.05	37.26 \pm 0.98	41.25 \pm 3.26
Non-adenoma	12	8.26 \pm 0.96	16.24 \pm 0.65	20.16 \pm 1.56
<i>t</i> value	—	18.518	70.814	21.785
<i>p</i> value	—	<0.001	<0.001	<0.001

TABLE 3. Conformity between the diagnostic results of the three examinations and the pathologic results (n).

Pathological findings		Dynamic contrast-enhanced MRI		Dynamic contrast-enhanced CT		Combined	
		Positive	Positive	Positive	Positive	Positive	Positive
Positive	56	45	11	46	10	55	1
Positive	12	2	10	2	10	2	10
Total	68	47	19	48	20	57	15

MRI: Magnetic Resonance Imaging; CT: computed tomography.

TABLE 4. Comparison of diagnostic efficacy of three methods (n, %).

Method	Sensitivity	Specificity	Accuracy	Positive predictive value	Negative predictive value
Dynamic contrast-enhanced MRI	80.36 (45/56)*	83.33 (10/12)	80.88 (55/68)*	95.74 (45/47)	47.62 (10/21)*
Dynamic contrast-enhanced CT	82.14 (46/56)*	83.33 (10/12)	82.35 (56/68)*	95.83 (46/48)	50.00 (10/20)*
Combined	98.21 (55/56)	83.33 (10/12)	95.59 (65/68)	96.49 (55/57)	90.91 (10/11)

*Compared with the combination of the two, * $p < 0.05$ indicates statistically significant differences. MRI: Magnetic Resonance Imaging; CT: computed tomography.*

TABLE 5. Results of ROC curve analysis.

Index	AUC	Standard error	<i>p</i> value	95% confidence interval	
				Upper limit	Lower limit
Dynamic contrast-enhanced MRI	0.818	0.062	<0.001	0.696	0.940
Dynamic contrast-enhanced CT	0.827	0.062	<0.001	0.706	0.949
Combined	0.908	0.057	<0.001	0.796	1.019

AUC: area under the curve; MRI: Magnetic Resonance Imaging; CT: computed tomography.

TABLE 6. Regional differences in paired samples under ROC curves.

Test results	Approximation		AUC Difference	Standard error difference	95% confidence interval approximation	
	<i>z</i>	<i>p</i> value			Upper limit	Lower limit
MRI-CT	-0.227	0.820	-0.009	0.343	-0.086	0.068
MRI-Joint	-3.458	0.001	-0.089	0.336	-0.140	-0.039
CT-Joint	-3.245	0.001	-0.080	0.335	-0.129	-0.032

AUC: area under the curve; MRI: Magnetic Resonance Imaging; CT: computed tomography.

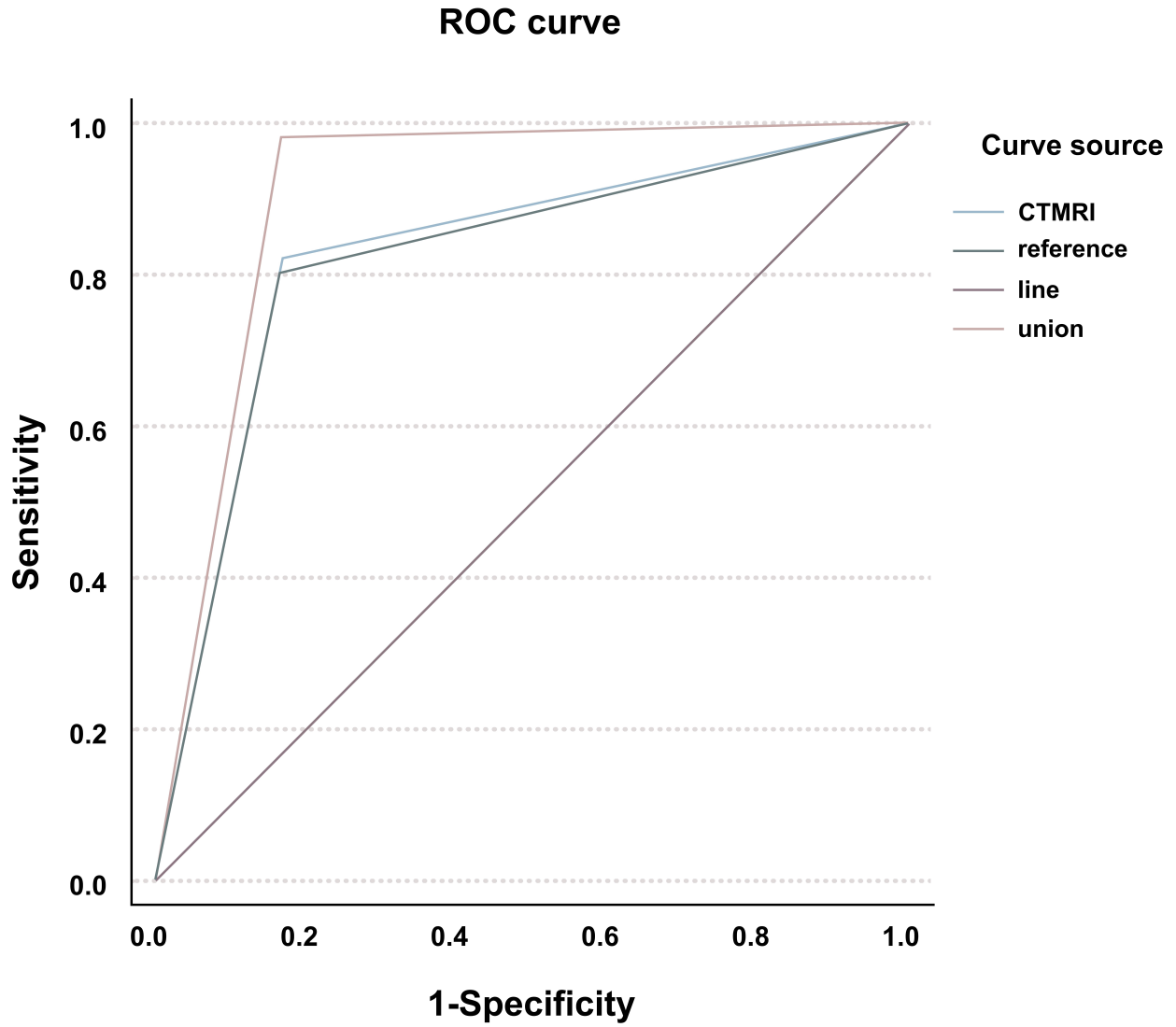


FIGURE 1. ROC curve analysis graph. ROC: receiver operating characteristic; CT: computed tomography; MRI: Magnetic Resonance Imaging.

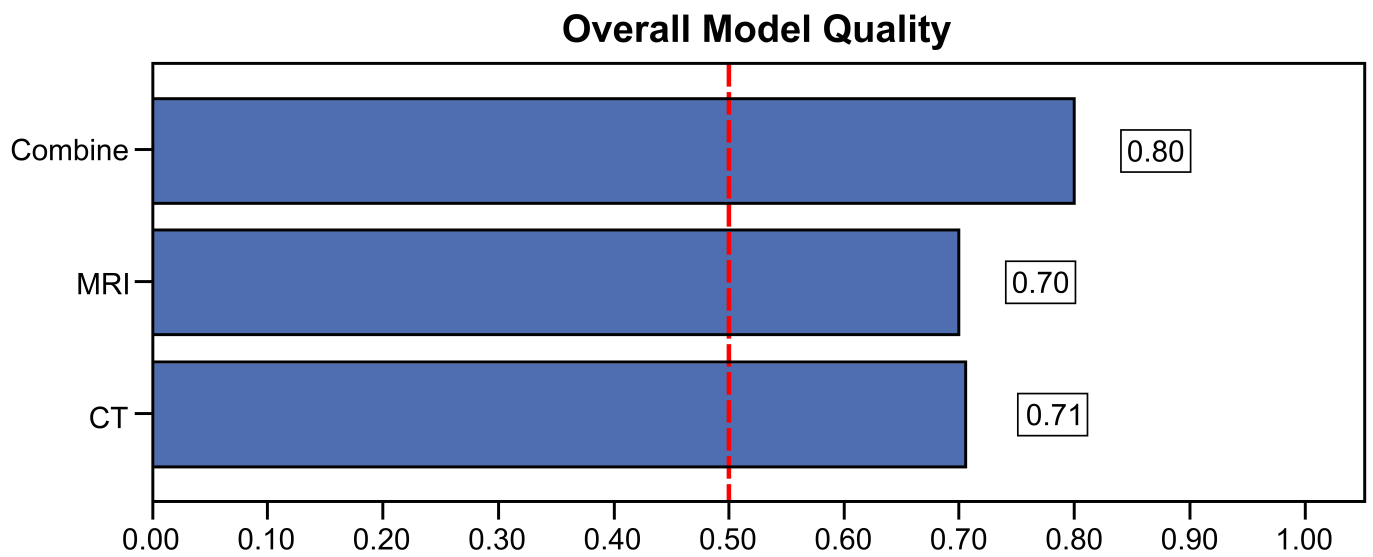


FIGURE 2. Overall model quality map. MRI: Magnetic Resonance Imaging; CT: computed tomography.

vessels and higher concentrations of lipid-rich hyalinocytes.

Compared to the separate examinations, the combined examination had significantly higher sensitivity, accuracy, and negative predictive value ($p < 0.05$). Based on the ROC curve, the combined diagnostics had the largest area under the curve, indicating a significant difference ($p < 0.05$). According to the results of the analysis of the overall quality of the model, the joint indexes were the largest. The combined diagnosis of the two appears to have the best effect and the highest predictive value. Combined diagnosis has some advantages over single diagnosis, mainly because CT is excellent for detecting and evaluating adrenal tumors [16–18]. It provides high-resolution images of the tumor that clearly show its size, shape, margins and internal structure. By using contrast agents, CT scans can also identify benign and malignant tumors by visualizing the blood supply of the tumor. Also, CT scans are usually faster and can be used in an emergency situation for a rapid diagnosis. Dynamic-enhanced CT is based on the rapid injection of a contrast agent through a vein, which is distributed to tissues and organs throughout the body through blood circulation. Successive scans at different time intervals allow the uptake, distribution and removal of the contrast agent from a specific organ or site to be observed. There can be differences in the distribution and metabolism of contrast agents between diseased and normal tissues. Normal and diseased tissues have different blood supply and vascular permeability, which can affect the rate of contrast agent aggregation, peak intensity, and clearance [14, 15]. A more detailed understanding of the blood supply of tissues and the enhancement characteristics of lesions can be gained by capturing and analyzing these dynamic change processes. This allows doctors to more accurately assess the lesions' nature, such as their benign and malignant nature, as well as their degree of activity. The analysis provides important basis for diagnosing, staging and developing treatment plans. It also provides a better understanding of the organ's functional status and other information. MRI plays a significant role in adrenal tumor evaluation. Due to MRI's high soft tissue contrast, tumor morphological features and internal structure are clearly visible. A variety of imaging sequences, including T1-weighted, T2-weighted, and enhancement scans, are available with MRI that help assess the tumor's nature and blood supply more comprehensively. Additionally, MRI can detect metastatic lesions and assess the tumor's relationship to surrounding structures. The combined examination is superior to individual tests due to their complementary strengths. Combining these two examinations is more helpful in diagnosing adrenal tumors and clarifying their nature. However, this study has the main drawback of a small number of participants, which limits the scope of statistical analysis. Results may be biased due to a small sample size, which limits their relevance to the general population. A single-center study reduced representativeness, as well. Furthermore, significant imaging information was withheld for reasons of patient confidentiality. Larger, multicenter, prospectively designed studies will be conducted in the future to validate and confirm these findings, as well as offer relevant imaging information.

5. Conclusions

In conclusion, the combination of dynamic-enhanced CT and dynamic-enhanced MRI is more effective at diagnosing adrenal tumors than either technique alone. Adrenal tumors can be diagnosed and treated more effectively when the two methods are combined, which has a wider clinical application.

AVAILABILITY OF DATA AND MATERIALS

The authors declare that all data supporting the findings of this study are available within the paper and any raw data can be obtained from the corresponding author upon request.

AUTHOR CONTRIBUTIONS

MHY—designed the study and carried them out. MHY, YNW—supervised the data collection, analyzed the data, interpreted the data. MHY and LHJ—prepared the manuscript for publication and reviewed the draft of the manuscript. All authors have read and approved the manuscript.

ETHICS APPROVAL AND CONSENT TO PARTICIPATE

Ethical approval was obtained from the Ethics Committee of Ningbo Yinzhou No.2 Hospital (Approval no. 2023024). Written informed consent was obtained from a legally authorized representative for anonymized patient information to be published in this article.

ACKNOWLEDGMENT

Not applicable.

FUNDING

This research received no external funding.

CONFLICT OF INTEREST

The authors declare no conflict of interest.

REFERENCES

- [1] Jing Y, Hu JB, Luo R, Mao Y, Luo ZX, Zhang MJ, *et al.* Prevalence and characteristics of adrenal tumors in an unselected screening population a cross-sectional study. *Annals of Internal Medicine.* 2022; 175: 1383–1391.
- [2] Prete A, Subramanian A, Bancos I, Chortis V, Tsagarakis S, Lang K, *et al.* Cardiometabolic disease burden and steroid excretion in benign adrenal tumors a cross-sectional multicenter study. *Annals of Internal Medicine.* 2022; 175: 325–334.
- [3] Schaafsma M, Berends AMA, Links TP, Brouwers AH, Kerstens MN. The diagnostic value of F-FDG PET/CT scan in characterizing adrenal tumors. *The Journal of Clinical Endocrinology and Metabolism.* 2023; 108: 2435–2445.
- [4] Mueller JW, Vogg N, Lightning TA, Weigand I, Ronchi CL, Foster PA, *et al.* Steroid sulfation in adrenal tumors. *The Journal of Clinical Endocrinology and Metabolism.* 2021; 106: 3385–3397.

- [5] Fassnacht M, Tsagarakis S, Terzolo M, Tabarin A, Sahdev A, Newell-Price J, *et al.* European society of endocrinology clinical practice guidelines on the management of adrenal incidentalomas, in collaboration with the European network for the study of adrenal tumors. *European Journal of Endocrinology*. 2023; 189: G1–G42.
- [6] Cui X, Hu D, Wang C, Chen S, Zhao Z, Xu X, *et al.* A surface-enhanced Raman scattering-based probe method for detecting chromogranin a in adrenal tumors. *Nanomedicine*. 2020; 15: 397–407.
- [7] Okamoto K, Ohno Y, Sone M, Inagaki N, Ichijo T, Yoneda T, *et al.* Should adrenal venous sampling be performed in PA patients without apparent adrenal tumors? *Frontiers in Endocrinology*. 2021; 12: 645395.
- [8] Nermoen I, Falhammar H. Prevalence and characteristics of adrenal tumors and myelolipomas in congenital adrenal hyperplasia: a systematic review and meta-analysis. *Endocrine Practice*. 2020; 26: 1351–1365.
- [9] Araujo-Castro M, Pascual-Corrales E, García Cano AM, Marchan M, Casals G, Hanzu FA, *et al.* Evaluation of body composition in patients with and without adrenal tumors and without overt hypersecretory syndromes. *Endocrine Practice*. 2023; 29: 110–118.
- [10] Zeng H, Wang X, Li H, Yang Q. Quantitative analysis of catecholamines and their metabolites in 491 patients with adrenal tumors: a retrospective single-center cohort study. *Journal of Cancer Research and Clinical Oncology*. 2023; 149: 4979–4989.
- [11] Ku EJ, Lee C, Shim J, Lee S, Kim KA, Kim SW, *et al.* Metabolic subtyping of adrenal tumors: prospective multi-center cohort study in Korea. *Endocrinology and Metabolism*. 2021; 36: 1131–1141.
- [12] Rees MA, Morin CE, Behr GG, Davis JC, Lai H, Morani AC, *et al.* Imaging of pediatric adrenal tumors: a COG diagnostic imaging committee/SPR oncology committee white paper. *Pediatric Blood & Cancer*. 2023; 70: e29973.
- [13] Ambroziak U. Approach to large adrenal tumors. *Current Opinion in Endocrinology, Diabetes and Obesity*. 2021; 28: 271–276.
- [14] Cambos S, Chanson P, Tabarin A. Analysis of steroid profiles by mass spectrometry: a new tool for exploring adrenal tumors? *Annales d'Endocrinologie*. 2021; 82: 36–42.
- [15] Ma GY, Zhang XJ, Wang MS, Xu XD, Xu BX, Guan ZW. Role of F-FDG PET/CT in the differential diagnosis of primary benign and malignant unilateral adrenal tumors. *Quantitative Imaging in Medicine and Surgery*. 2021; 11: 2013–2018.
- [16] Alimu P, Fang C, Han Y, Dai J, Xie C, Wang J, *et al.* Artificial intelligence with a deep learning network for the quantification and distinction of functional adrenal tumors based on contrast-enhanced CT images. *Quantitative Imaging in Medicine and Surgery*. 2023; 13: 2675–2687.
- [17] Zdrojewska M, Mech-Siebieszuk E, Swiatkowska-Stodulska R, Regent B, Kunc M, Zdrojewski L, *et al.* Adrenal tumors in young adults: case reports and literature review. *Medicina*. 2022; 58: 746.
- [18] Yanagisawa M, Malik DG, Loehfelm TW, Fananapazir G, Corwin MT, Campbell MJ. Adrenal tumors found during staging and surveillance for colorectal cancer: benign incidentalomas or metastatic disease? *World Journal of Surgery*. 2020; 44: 2282–2287.

How to cite this article: Minghui Yan, Yanan Wang, Lianghong Jiao. Comparative analysis of dynamic contrast-enhanced MRI, dynamic contrast-enhanced CT, and their combination for adrenal tumor diagnosis in men. *Journal of Men's Health*. 2024; 20(7): 113-119. doi: 10.22514/jomh.2024.115.